Continuous Under-Frequency Load Shedding Scheme for Power System Adaptive Frequency Control

Changgang Li, *Member*, *IEEE*, Yue Wu, Yanli Sun, Hengxu Zhang, *Member*, *IEEE*, Yutian Liu, *Senior Member*, *IEEE*, Yilu Liu, *Fellow*, *IEEE*, and Vladimir Terzija, *Fellow*, *IEEE*

***Abstract*—Frequency drop due to loss of massive generation is a threat to power system frequency stability. Under-frequency load shedding (UFLS) is the principal measure to prevent successive frequency declination and blackouts. Based on traditional stage-by-stage UFLS scheme, a new continuous UFLS scheme is proposed in this paper to shed loads proportional to frequency deviation. The characteristic of the proposed scheme is analyzed with a closed-form solution of frequency dynamics. Frequency threshold and time delay are added to make the proposed scheme practical. A line-by-line scheme based on precise load control is introduced to implement the continuous scheme for systems without enough continuously controllable loads. The load shedding scale factor of the proposed scheme is tuned with an analytical method to achieve adaptability to different operating conditions. The adaptability of the proposed scheme is validated with 39-bus New England model and simplified Shandong Power Grid of China.**

***Index Terms*—Power systems, frequency stability, under-frequency load shedding (UFLS), continuous control, precise load control**

I. INTRODUCTION

FREQUENCY is an essential index of balance between active power generation and load. Frequency will drop if active power generation is inadequate due to loss of generation in large-scale power systems [1] or microgrids [2]. Large frequency excursion may lead to system blackouts and restoration failure [3]. Systems with more integration of intermittent renewable generation are more vulnerable to frequency deviation [4][5]. It is compulsory to arrest frequency declination for preventing power systems from severe consequences. The key technique to recover frequency in under-frequency scenarios is under-frequency load shedding (UFLS) which rebalances generation and load by shedding appropriate amount of loads.

UFLS can be generally classified into three categories: traditional stage-by-stage scheme, adaptive scheme, and semi-adaptive scheme [6]. The major difference between the three schemes lies in the method to determine load shedding amount. For the stage-by-stage scheme, the loads to shed are predefined and divided into several stages. Each stage is tripped when frequency drops beyond a certain threshold for a few seconds. It sheds loads based on local frequency and is widely used in utilities [7]. Difference between the frequency thresholds of stages must be set to overcome oscillation between generators. The typical frequency difference between stages is 0.2~0.25Hz, and 5~8 stages are usually set. The time delay is adaptively adjusted according to frequency dynamics in [8] to improve scheme adaptability. In [9] and [10], the stage-by-stage scheme is optimized with trigger signal of both frequency deviation and rate of change of frequency (ROCOF). Uncertainty of system parameters is considered in [11] to tune more adaptive scheme. Though the stage-by-stage scheme can be tuned for better adaptability, the limited stages and inherent discreteness make it hard to set up a scheme suitable for all possible operating conditions. Over-shedding or under-shedding problem can hardly be avoided for the stage-by-stage scheme [12].

For the adaptive scheme, the loads to shed are calculated online based on ROCOF of the center of inertia (COI). It is derived from the fact that the initial ROCOF of COI is proportional to power imbalance [13]. Therefore, loads equal to the product of ROCOF and system inertia are shed to balance generation and load in one shot. In [14], load shedding amount is distributed to different loads considering voltage stability and power tracing criteria. The adaptive scheme is improved in [15] considering change of power generation during load shedding process. The difference between measured ROCOF and threshold of ROCOF is adopted in [16] for determining appropriate load shedding amount. The calculation of ROCOF of COI requires wide area measurement data from different locations. Communication channels with high availability are prerequisite of the adaptive scheme for estimating power imbalance and sending load shedding command. Biased estimation of ROCOF or system inertia further prevents it from industrial applications.

Semi-adaptive scheme adopts both ROCOF and frequency deviation to determine loads to shed [17]. It can be treated as a combination of the stage-by-stage scheme and adaptive scheme. In the first stage, loads to shed are calculated based on measured ROCOF of COI, like the adaptive scheme. For other stages, loads are predefined and shed according to frequency deviation. The semi-adaptive scheme is not immune to over-shedding or under-shedding problem due to the similarly limited stages as the stage-by-stage scheme.

This work was supported by National Key R&D Program of China (No: 2017YFB0902600), National Science Foundation of China (No: 51407107), and Young Scholars Program of Shandong University (No: 2018WLJH31).

Changgang Li, Yue Wu, Yanli Sun, Hengxu Zhang and Yutian Liu are with the Key Laboratory of Power System Intelligent Dispatch and Control of the Ministry of Education (Shandong University), Jinan, 250061 China (e-mail: liuyt@sdu.edu.cn).

Yilu Liu is with the Department of Electrical Engineering and Computer Science, University of Tennessee, Knoxville, TN 37996, USA (e-mail: liu@utk.edu).

Vladimir Terzija is with the School of Electrical and Electronic Engineering, the University of Manchester, Manchester, UK M60 1QD. (e-mail: vladimir.terzija@manchester.ac.uk)

A new continuous UFLS scheme is proposed in this paper to adaptively determine loads to shed while overcoming the drawbacks of existing schemes. The main contributions of this paper are three-fold. Firstly, the concept of continuous UFLS is proposed, and it is proved analytically that the proposed scheme is adaptive to different operating conditions and events, and immune to the over-shedding problem. Secondly, non-linear factors of frequency threshold and time delay are considered to improve the continuous UFLS scheme for applicability. A line-by-line scheme with precise load control is proposed to implement the continuous UFLS scheme. Thirdly, a tuning method is proposed to set up the load shedding scale factor of the continuous UFLS scheme. The proposed continuous UFLS scheme and tuning method are verified to be valid to bring system frequency back.

The rest of this paper is organized as follows. The basic idea of the continuous UFLS scheme is proposed in section II, and its property is analyzed with system frequency response (SFR) model. Impact of such nonlinear factors as spinning reserve, frequency threshold, and time delay is analyzed in section III, and the continuous UFLS scheme is improved with frequency threshold and time delay. Practical implementation of the proposed scheme with precise load control is also discussed in section III. A method to tune the proposed continuous UFLS scheme is introduced in section IV. With the 39-bus New England model and simplified Shandong Power Grid of China, the performance of the continuous UFLS scheme is further verified in section V with different events and operating conditions. Discussions on the limitation and possible applications of the proposed scheme are made in section VI, and conclusions are drawn in section VII.

II. The Basis of Continuous UFLS Scheme

A. From discrete scheme to continuous scheme

Some methods were proposed to increase the number of stages for a smoother stage-by-stage scheme and better performance. Ignoring oscillation, Fig. 1 shows two stage-by-stage schemes where P_{LS} is load shedding amount and Δf is frequency deviation. One is the solid line with five stages, and the other is the dot-dashed line with 12 stages. Scheme with more stages is more adaptive to different operating conditions than schemes with fewer stages [9]. If the number of stages is increased to infinite, the load shedding curve will become continuous as the dashed line in Fig. 1.

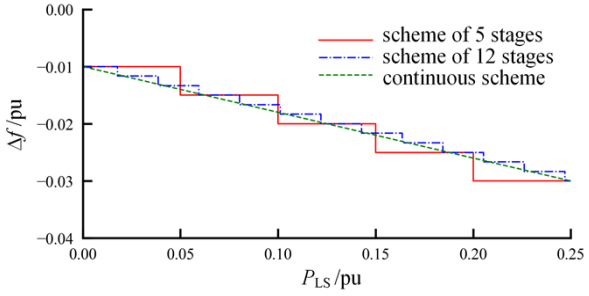

Fig. 1 Traditional stage-by-stage schemes with different stages and continuous UFLS scheme

In the continuous UFLS scheme, the load shedding amount is determined online with frequency deviation as:

$$P_{LS} = -K_{LS}\Delta f \tag{1}$$

where K_{LS} is load shedding scale factor to tune.

Equation (1) shows the basic idea of continuous UFLS scheme in which loads are shed continuously. With loads continuously shed with (1), it is supposed to be adaptive to different operating conditions and is analyzed as follows.

B. SFR model with continuous UFLS scheme

System frequency is complicated in real power systems. To investigate the general performance of the proposed continuous UFLS scheme, SFR model proposed in [18] is adopted in this paper. Method to get the equivalent parameters for SFR can be found in [19]. It should be noted that the SFR model is simplified to examine the frequency dynamics of a system dominated by steam-turbine generators. Complex dynamics such as limited spinning reserve and boiler dynamics are neglected. The results of the SFR model can only be used to check the general performance of the proposed UFLS scheme.

Fig. 2 shows the diagram of SFR model, where P_D is the amount of power imbalance due to event, H is system inertia, D is system damping consisting of both damping of generator and load frequency dependency, R is droop of governor, F_H is the fraction of mechanical power generated by high-pressure cylinder, T_R is time constant of reheater, and K_m is gain of mechanical power. The continuous UFLS scheme is added in the dashed box of Fig. 2.

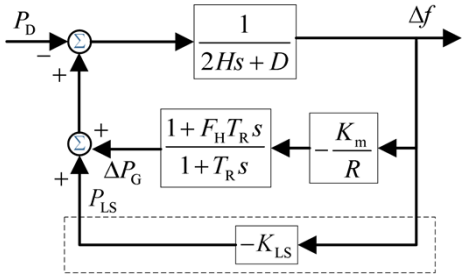

Fig. 2 Modified SFR model with continuous UFLS scheme

Though K_{LS} works as feedback control and looks like load frequency control or load frequency dependency, it is different from the other two. The major difference lies in the fact that the loads shed with K_{LS} are disconnected by tripping transmission lines and will not be immediately restored when frequency is recovered. The dispatching command to recover the shed loads should be given according to guidelines only when the system is successfully recovered from the severe disturbance.

Based on the analysis made in [18], the system frequency deviation before reaching its nadir can be expressed as the following frequency-domain equation:

$$\Delta f(s) = \frac{-RP_D\omega_n^2}{D_e}\frac{1+T_R s}{\left(s^2+2\delta\omega_n s+\omega_n^2\right)s} \tag{2}$$

where D_e is equivalent damping, ω_n is natural oscillation frequency and δ is damping ratio. D_e, ω_n, and δ are defined as:

$$\begin{cases} D_e = K_m + (D + K_{LS})R \\ \omega_n^2 = \dfrac{D_e}{2HRT_R} \\ \delta = \dfrac{2HR + (D+K_{LS})RT_R + K_m F_H T_R}{2D_e}\omega_n \end{cases} \tag{3}$$

In [18], the analytic time-domain expression of Δf was built as two equations separately depending on δ. A uniform expression of system frequency is derived in this paper to make the model consistent as:

$$\Delta f(t)=\frac{-RP_{\mathrm{D}}}{D_{\mathrm{e}}}\left[\frac{c_1\left(e^{\lambda_1 t}-1\right)}{\lambda_1}+\frac{c_2\left(e^{\lambda_2 t}-1\right)}{\lambda_2}\right] \tag{4}$$

where

$$\lambda_1=-\delta\omega_{\mathrm{n}}-\omega_{\mathrm{n}}\sqrt{\delta^2-1},\quad \lambda_2=-\delta\omega_{\mathrm{n}}+\omega_{\mathrm{n}}\sqrt{\delta^2-1} \tag{5}$$

$$c_1=\frac{\omega_{\mathrm{n}}^2\left(1+T_{\mathrm{R}}\lambda_1\right)}{\lambda_1-\lambda_2},\qquad c_2=\frac{\omega_{\mathrm{n}}^2\left(1+T_{\mathrm{R}}\lambda_2\right)}{\lambda_2-\lambda_1} \tag{6}$$

If the system is over-damped with δ>1.0, λ_1 and λ_2 are real numbers and the system frequency response can be readily obtained. If the system is under-damped with δ<1.0, λ_1 and λ_2 become complex conjugate numbers. It can be proved that the two parts within the bracket of (4) are conjugate of each other. Therefore, equation (4) always give real frequency response in both under and over damped cases.

When frequency reaches its minimum, the derivative of Δf over t is 0. Therefore, it can be derived from (4) that the time when frequency reaches its minimum is;

$$t_{\min}=\frac{1}{\lambda_2-\lambda_1}\ln\frac{1+T_{\mathrm{R}}\lambda_1}{1+T_{\mathrm{R}}\lambda_2} \tag{7}$$

C. *Characteristic of continuous UFLS scheme*

With the frequency response of (4), some characteristic of the proposed continuous UFLS scheme can be found as follows.

1) Load shedding amount is proportional to initial power imbalance, and the continuous scheme is adaptive to different events.

The total amount of shed load is the product of K_{LS} and $\Delta f_{\min}$, i.e., the minimum frequency at $t_{\min}$. $\Delta f_{\min}$ can be expressed as:

$$\begin{aligned}\Delta f_{\min}&=-\frac{RP_{\mathrm{D}}}{D_{\mathrm{e}}}\left[\frac{c_1\left(e^{\lambda_1 t_{\min}}-1\right)}{\lambda_1}+\frac{c_2\left(e^{\lambda_2 t_{\min}}-1\right)}{\lambda_2}\right]\\&=-\frac{RP_{\mathrm{D}}}{D_{\mathrm{e}}}\left\{\frac{c_1}{\lambda_1}\left[\left(\frac{-c_1}{c_2}\right)^{\frac{\lambda_1}{\lambda_2-\lambda_1}}-1\right]+\frac{c_2}{\lambda_2}\left[\left(\frac{-c_1}{c_2}\right)^{\frac{\lambda_2}{\lambda_2-\lambda_1}}-1\right]\right\}\\&=MP_{\mathrm{D}}\end{aligned} \tag{8}$$

where M is a constant scale factor between $\Delta f_{\min}$ and P_{D}:

$$M=-\frac{R}{D_{\mathrm{e}}}\left\{\frac{c_1}{\lambda_1}\left[\left(\frac{-c_1}{c_2}\right)^{\frac{\lambda_1}{\lambda_2-\lambda_1}}-1\right]+\frac{c_2}{\lambda_2}\left[\left(\frac{-c_1}{c_2}\right)^{\frac{\lambda_2}{\lambda_2-\lambda_1}}-1\right]\right\} \tag{9}$$

Therefore, the total load shedding amount is:

$$P_{\Sigma\mathrm{LS}}=-K_{\mathrm{LS}}\Delta f_{\min}=-K_{\mathrm{LS}}MP_{\mathrm{D}}=CP_{\mathrm{D}} \tag{10}$$

where C is:

$$C=\frac{R}{D_{\mathrm{e}}}\left\{\frac{c_1}{\lambda_1}\left[\left(\frac{-c_1}{c_2}\right)^{\frac{\lambda_1}{\lambda_2-\lambda_1}}-1\right]+\frac{c_2}{\lambda_2}\left[\left(\frac{-c_1}{c_2}\right)^{\frac{\lambda_2}{\lambda_2-\lambda_1}}-1\right]\right\}K_{\mathrm{LS}} \tag{11}$$

C is a parameter determined by system configuration and K_{LS}. It is independent of disturbance and is a constant for a certain system with specific K_{LS}.

It can be concluded from (10) and (11) that the total shed load is proportional to the initial power imbalance. When system parameters and K_{LS} are fixed, the continuous scheme will shed loads proportional to the power imbalance, i.e., the continuous scheme is adaptive to different events.

2) Load shedding amount is always less than power imbalance and C<1.0. The continuous scheme is immune to over-shedding problem.

As discussed in (7), the derivative of Δf over t is 0 at $t_{\min}$. Therefore, the swing equation at $t_{\min}$ can be expressed as:

$$\left.\frac{d\Delta f}{dt}\right|_{t_{\min}}=\frac{1}{2H}\left(-P_{\mathrm{D}}+\Delta P_{\mathrm{G}}+P_{\Sigma\mathrm{LS}}-D\Delta f_{\min}\right)=0 \tag{12}$$

and the expression of total load shedding amount is:

$$P_{\Sigma\mathrm{LS}}=P_{\mathrm{D}}-\Delta P_{\mathrm{G}}+D\Delta f_{\min} \tag{13}$$

where ΔP_{G} is the change of mechanical power due to primary frequency regulation.

Since Δf is negative and ΔP_{G} is positive in under-frequency scenarios, it can be concluded that:

$$P_{\Sigma\mathrm{LS}}<P_{\mathrm{D}} \tag{14}$$

It indicates that the total shed load with the continuous UFLS scheme is always less than power imbalance. In other words, there is no over-shedding problem for the continuous UFLS scheme. It can also be concluded from (10) that the constant C is always less than 1.0.

Simulations are carried out on the SFR model to investigate the impact of K_{LS} on load shedding amount with parameters from [18], i.e., H=4s, T_{R}=8s, D=1, F_{H}=0.3, K_{m}=0.95, R=0.05. With an event of P_{D}=0.2, the relationship between C and K_{LS} is shown in Fig. 3.

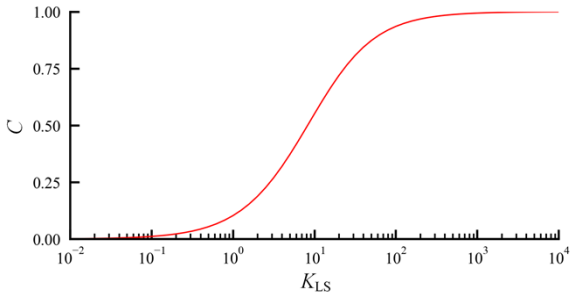

Fig. 3 The relationship between load shedding factor C and K_{LS}

It can be verified from Fig. 3 that the total load shedding amount is increasing with K_{LS}. Saturation can be observed in Fig. 3 that, C increases quickly when K_{LS} increases in the range of (0, 100), and C is less sensitive to K_{LS} while K_{LS} is greater than 100. C is approaching to 1.0 when K_{LS} is infinite. Therefore, the load shedding amount with the continuous UFLS scheme is always less than the power imbalance no matter how K_{LS} is tuned. In other words, Fig. 3 is consistent with (14) and there is no over-shedding problem for the continuous UFLS scheme.

III. Improved Continuous UFLS Scheme with Nonlinear Factors

The SFR model is greatly simplified to be linear. However, there are obvious nonlinear factors in practical cases where the analytical property in section II is not applicable. In this section, nonlinear factors of spinning reserve, frequency threshold, and

time delay are investigated, and an improved continuous UFLS scheme is proposed.

A. Impact of spinning reserve

Spinning reserve is the available generation that can be increased in a short time to meet load variation. Spinning reserve is usually limited to a small portion of total generation to balance the requirements of stability and economy. Simulations are carried out with different spinning reserve levels as shown in Fig. 4 with K_{LS}=20 and P_D=0.2 to check the impact of spinning reserve on frequency dynamics.

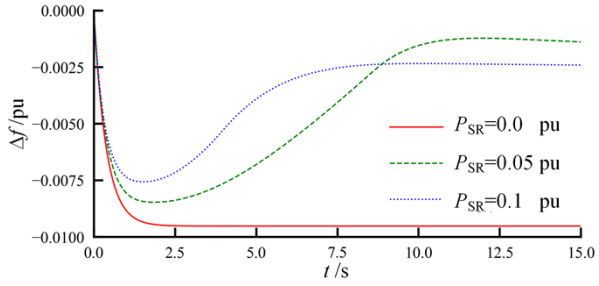

Fig. 4 Frequency response with different levels of spinning reserve

It can be found from Fig. 4 that frequency is stalling when there is no spinning reserve. It can be proved with (13) that, without change of mechanical power, the shed load will not bring system frequency back and the system residual frequency deviation is $-P_D/(D+K_{LS})$. When the spinning reserve is 5%, system frequency deviation can quickly be recovered to about –0.001pu. Comparing cases when the spinning reserve is 5% and 10%, it can be found that more spinning reserve does not necessarily lead to less frequency deviation due to nonlinearity. The minimum frequency which determines the total load shedding amount is greater in the case with 5% of spinning reserve. It then leads to more shed loads than the case with 10% of spinning reserve and less residual frequency deviation.

B. Impact of frequency threshold

Under normal operating conditions, loads are continually varying, and frequency cannot be exactly held at nominal value. According to operating guides, frequency deviation under normal operating conditions should be limited in a small range, e.g., less than ±0.2Hz, and regulated by primary and secondary frequency regulation. In such circumstance, loads should not be shed. Therefore, appropriate frequency threshold should be set to avoid shedding loads unintendedly. The frequency threshold for UFLS is different among different balancing authorities. For example, the frequency threshold is 59.5Hz in Northeast Power Coordinating Council (NPCC), 59.3Hz in Mid Continent Area Power Pool (MCAPP), and 59.1Hz in Western Electricity Coordinating Council (WECC). In China, the frequency threshold is usually set as 49.5Hz.

The continuous UFLS scheme is updated to model the frequency threshold, and actual load shedding amount is determined in (15) where Δf_{th} is the threshold of frequency deviation in per unit.

$$P_{LS}=\begin{cases}0 & \text{if } \Delta f > \Delta f_{th}\\ -K_{LS}\left(\Delta f-\Delta f_{th}\right) & \text{if } \Delta f < \Delta f_{th}\end{cases} \quad (15)$$

With K_{LS}=20 and P_D=0.2, the frequency response with different frequency threshold is shown in Fig. 5. It can be found from Fig. 5 that, with greater frequency threshold, the maximum frequency deviation becomes greater, and lower residual frequency can be observed. System frequency performance is deteriorated with greater frequency threshold. It is necessary to tune K_{LS} to be greater for systems with greater frequency threshold to prevent severe frequency drop and recover frequency to a high level.

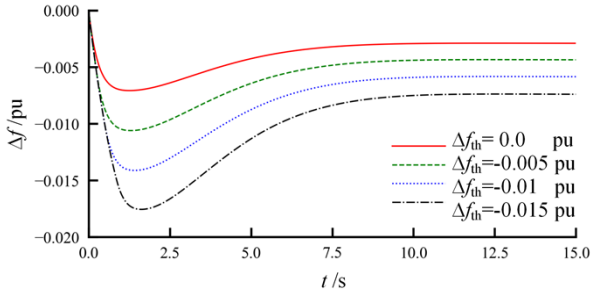

Fig. 5 Frequency response with different frequency thresholds

Furthermore, since the transient frequency nadir is always less than the frequency threshold, (13) can be modified as:

$$P_D - P_{\Sigma LS} = -D\Delta f_{min} + \Delta P_G \geqslant -D\Delta f_{min} > -D\Delta f_{th} \quad (16)$$

It is indicated by (16) that, the shortage of load shedding amount is always greater than $-D\Delta f_{th}$. In order to make the load shedding amount as close as the initial power imbalance, it is necessary to shed additional loads greater than $-D\Delta f_{th}$ without risk of over-shedding. The additional loads to shed are called additional stage in this paper with P_{add} and t_{add} denoting the load shedding amount and time delay of the additional stage.

An example is given in Fig. 6 to show the logic of the additional stage. The states of the additional stage, a.k.a. *s* in Fig. 6, are "wait", "trigger" and "shed". When frequency deviates from Δf_{th}, a historic minimum frequency recorder is initiated to store the minimum value of the following frequency dynamics. The additional stage is in the "wait" state when the historic minimum frequency is declining. It turns into "trigger" state and the timer of the additional stage is started when the historic minimum frequency stops changing. If the historic minimum frequency holds for t_{add}, the timer is timed out and the additional stage will be in "shed" state to trip loads. Otherwise, the timer will be reset and the additional stage will return to "wait" state. Once frequency recovers above Δf_{th}, the historic minimum frequency record is cleared.

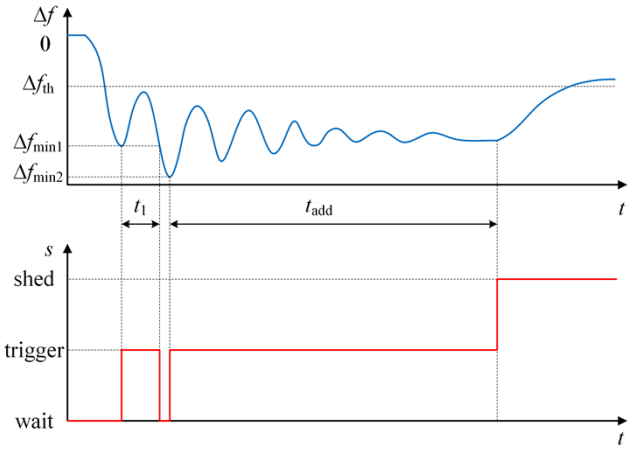

Fig. 6 The logic of the additional stage

C. Impact of time delay

Traditional stage-by-stage scheme usually shed loads with appropriate time delay t_d to filter out temporary frequency drop and make sure different stages are shed in sequence. It is compulsory for the frequency to drop beyond threshold frequency for the delayed time before loads are tripped. The typical time delay is 0.1~0.3s. In this paper, t_d is selected as 0.2s.

An appropriate time delay is also necessary for the proposed continuous UFLS scheme. A general way to implement the time delay is to calculate the loads to shed with measured frequency and start a timer immediately. Loads are then shed once the timer is timed out. However, the system may suffer the over-shedding problem in cases that frequency has already been recovered before the timer is timed out. The logic of time delay is then improved by adding logic as follows to overcome the over-shedding problem:

$$P_{LS}(t)=\begin{cases} P_{LS}^{c} & \text{if } \dfrac{d\Delta f}{dt}<0 \text{ and } P_{LS}^{c}>P_{LS}^{t} \\ P_{LS}^{t} & \text{if } \dfrac{d\Delta f}{dt}\geq 0 \text{ or } P_{LS}^{c}\leq P_{LS}^{t} \end{cases} \quad (17)$$

where P^t_{LS} is the loads that has already been shed corresponding to the historic minimum frequency, and P^c_{LS} can be calculated by the following equation:

$$P_{LS}^{c}=-K_{LS}\left[\Delta f(t-t_d)-\Delta f_{th}\right] \qquad \Delta f<\Delta f_{th} \quad (18)$$

The recovery of frequency is an indicator of enough load shedding amount. In the improved logic (17), the loads are shed only when the timer is timed out and frequency is still declining. The total shed amount is determined by the frequency at the time which is t_d before t_{min}. In other words, the total shed amount is less than the one calculated with Δf_{min}. Therefore, the time delay will not introduce the over-shedding problem which can be verified with (16).

Simulation result with K_{LS}=20 and P_D=0.2 is shown in Fig. 7 to check the impact of time delay. It is clear that the frequency nadir is dropped with a longer time delay. However, the impact of time delay on residual frequency can be overlooked when t_d<0.2s.

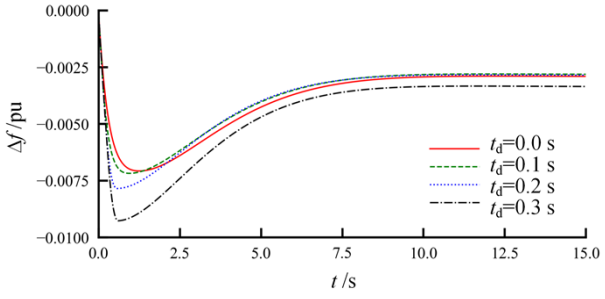

Fig. 7 Frequency response with different time delay

D. Improved continuous UFLS scheme and examination

With the previous discussion, an improved continuous UFLS scheme is illustrated in the dashed box of Fig. 8 to include nonlinearity. In Fig. 8, P_{max} and P_{min} are upper and lower bound of generation. The output of recovered logic is 0 if frequency is declining and 1 if frequency is recovered.

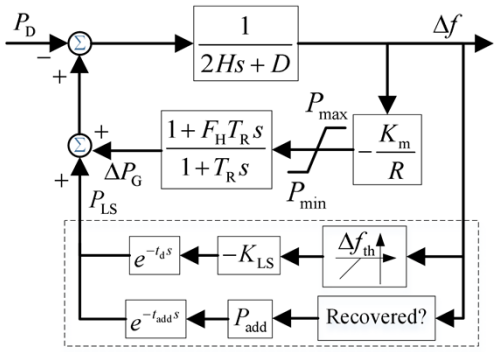

Fig. 8 Extended SFR model with continuous UFLS scheme including frequency threshold, time delay and additional stage

An example is set with K_{LS}=35, Δf_{th}=−0.01, t_d=0.2s, and P_{SR}=5% to compare the performance of the improved continuous UFLS scheme and the ideal scheme in section II. Additional stage is set as P_{add}=1% and t_{add}=10s. The relationship between total load shedding amount and power imbalance is shown in Fig. 9.

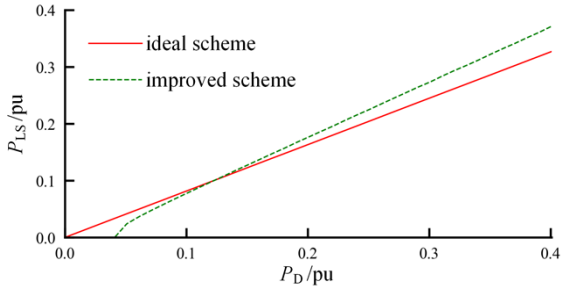

Fig. 9 Comparison between ideal and improved continuous UFLS schemes with different events

It can be seen from Fig. 9 that the total load shedding amount is increasing with disturbance for the improved scheme. However, when disturbance is less than 0.044, no load is shed with the improved scheme since frequency recovers before dropping beyond Δf_{th}. With limited spinning reserve, total load shedding amount of the improved scheme is greater than the ideal scheme when disturbance is greater than 0.123 since the frequency nadir is greatly dropped.

Fig. 10 shows the relationship between total load shedding amount and K_{LS} with P_D=0.2 and the same Δf_{th}, t_d, P_{SR}, P_{add}, and t_{add} as Fig. 10. It can be found from Fig. 10 that the total load shedding amount is greater for the improved UFLS scheme when K_{LS}<60 due to greater frequency deviation. With frequency threshold, the total load shedding amount of the improved scheme will not reach power imbalance even K_{LS} approaches infinite. There is no over-shedding problem for the improved continuous UFLS scheme.

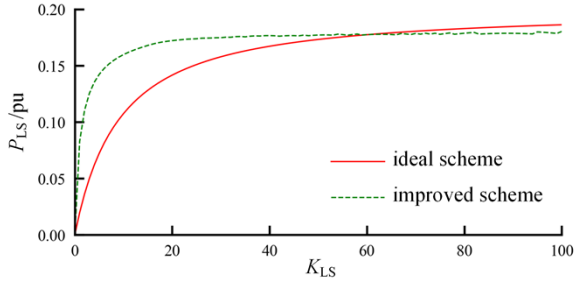

Fig. 10 Comparison between ideal and improved continuous UFLS schemes with different K_{LS}

It can be summarized that the performance of improved continuous UFLS scheme is nonlinear when spinning reserve, frequency threshold, and time delay are considered. However, the dominant characteristic of the UFLS scheme is kept, e.g., the load shedding amount is increasing with greater K_{LS} and is almost proportional to power imbalance.

E. Implementation with precise load control

The proposed continuous UFLS scheme is dependent on loads with high controllability which can be achieved with smart power electronic controllers, such as energy storage systems [20]. However, the amount of loads with such controllability is not enough for emergency frequency control in most power systems nowadays.

Traditional stage-by-stage scheme sheds loads by tripping lines of high voltage level, and massive loads will be shed if one line is tripped. Current advancement of communication technology enables such applications as fast demand side management [21] and precise load control [22]. It provides a precise way to trip lines of lower voltage level other than tripping lines of high voltage level. The load shedding amount can be approximated as continuous if lines of lower voltage level are tripped one by one.

With precise load control, the proposed UFLS scheme can be implemented with a line-by-line scheme in one of two modes: local and remote, as shown in Fig. 11. In the local mode, UFLS signal is generated in substation and then sent to circuit breakers (CBs) inside the substation. In the remote mode, UFLS signal is also generated in substation but sent to CBs of lower voltage level via additional communication channels. Load shedding amount is calculated in the substation with local frequency and a minimum amount of lines to provide enough load to shed is then determined according to line priority. When the frequency is declining, the increasing load shedding command is transformed into tripping signals for lines of lower voltage level and sent to breakers via communication channels to shed loads gradually.

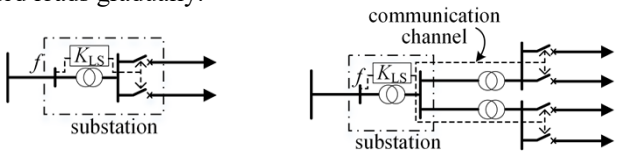

(a) local mode (b) remote mode

Fig. 11 Line-by-line UFLS scheme based on continuous UFLS scheme

If loads are shed in remote mode, the number of lines of lower voltage level is large and the load shedding is almost continuous. However, in some systems with many large factories, a large portion of loads is directly connected to high-voltage lines. Tripping loads on lower voltage lines may be insufficient to bring frequency back. In this case, CBs on some high-voltage lines should be further tripped in local mode. Since the load on the high-voltage line is heavy, tripping high-voltage lines may deteriorate the continuity of the proposed UFLS scheme. The performance of the line-by-line scheme is further examined in section V.

IV. TUNING OF CONTINUOUS UFLS SCHEME

A. The requirement of tuning K_{LS}

Suppose the greatest active power deficiency is P_{Dmax}, the K_{LS} should be tuned to make sure the residual frequency can be successfully recovered above Δf_{th}. Though greater K_{LS} leads to more load to shed and less frequency deviation, K_{LS} cannot be tuned as infinite in field applications due to several reasons.

Firstly, frequency is always measured with bias. Greater K_{LS} leads to more shed loads with a small change of frequency. To shed the precise amount of loads, it requires frequency measurement devices with high accuracy. Secondly, results in Fig. 4 indicate that the total load shedding amount is not sensitive to the change of K_{LS} when K_{LS} is great enough. It is reasonable to select K_{LS} as little as possible while preventing the system from frequency instability. Thirdly, t_{min} is usually quite small for specific events. If the continuous UFLS scheme is implemented with controllable loads, loads need to change greatly in a short time if K_{LS} is too great. It may be impossible for some devices of which the maximum power change rate is limited by controllers.

B. Tuning of K_{LS} with constant damping

It can be readily concluded that the frequency would drop most if the power imbalance is P_{Dmax} when there is no spinning reserve. Without spinning reserve, the system minimum frequency Δf_{min} is equal to the residual frequency Δf_{∞}. Therefore, if no additional stage is considered, the power balance equation when the system is stabilized can be modeled as:

$$\left(1-P_{D\max}\right)-\left(1+K_{LS}\Delta f_{\min}\right)-D\Delta f_{\min}=0 \tag{19}$$

or

$$K_{LS}=-\frac{P_{D\max}}{\Delta f_{\min}}-D \tag{20}$$

If the frequency threshold and additional stage are further considered, the minimum frequency before the additional stage is shed can be calculated with:

$$\left(1-P_{D\max}\right)-\left[1+K_{LS}\left(\Delta f_{\min}-\Delta f_{th}\right)\right]-D\Delta f_{\min}=0 \tag{21}$$

After the additional stage is shed, the power balance when the residual frequency is reached is:

$$\left(1-P_{D\max}\right)-\left[1+K_{LS}\left(\Delta f_{\min}-\Delta f_{th}\right)+D\Delta f_{th}\right]-D\Delta f_{\infty}=0 \tag{22}$$

From (21) and (22), it can be calculated that,

$$\Delta f_{\min}=\Delta f_{th}+\Delta f_{\infty} \tag{23}$$

Substitute (23) into (21), the K_{LS} can be obtained as:

$$K_{LS}=-\frac{P_{D\max}+D\left(\Delta f_{th}+\Delta f_{\infty}\right)}{\Delta f_{\infty}} \tag{24}$$

For the worst case with $\Delta f_{\infty}=\Delta f_{th}$, the minimum K_{LS} is:

$$K_{LS\min}=-\frac{P_{D\max}+2D\Delta f_{th}}{\Delta f_{th}} \tag{25}$$

If P_{Dmax}=0.3, Δf_{th}=–0.01, and D=1, K_{LSmin} can be readily calculated as 28 from (25). When K_{LS}=28, Δf_{min} is –0.02pu from (23) which is –1Hz for 50Hz systems or –1.2Hz for 60Hz systems. Tuning K_{LS} to be greater than K_{LSmin} will bring system frequency back to higher than Δf_{th}.

C. Tuning of K_{LS} with varying damping

In most power systems, D is mainly contributed by load frequency dependency, which is mostly determined by motors. When part of loads is shed, the system damping is also reduced, and system frequency performance is deteriorated [23]. To deeper look into the effect of varying damping on system

frequency control, a load model with frequency dependency and load shedding is considered as:

$$P_{\mathrm{L}} = P_{\mathrm{L0}}\left(1+D\Delta f\right)\left(1-P_{\Sigma\mathrm{LS}}\right) \tag{26}$$

where P_{L} is load power and P_{L0} is nominal load power. With initial nominal load power as base power, P_{L0} is 1.0 p.u.

When there is no spinning reserve and frequency threshold and additional stage are not considered, the power balance can be modeled as following which is similar to (19):

$$\left(1-P_{\mathrm{Dmax}}\right)-\left(1+K_{\mathrm{LS}}\Delta f_{\min}\right)\left(1+D\Delta f_{\min}\right)=0 \tag{27}$$

and K_{LS} can be derived as:

$$K_{\mathrm{LS}} = \frac{-P_{\mathrm{D\,max}} - D\Delta f_{\min}}{\Delta f_{\min}\left(1+D\Delta f_{\min}\right)} \tag{28}$$

If frequency threshold is further considered when there is no spinning reserve, power balance at $t_{\min}$ is:

$$\left(1-P_{\mathrm{D\,max}}\right)-\left[1+K_{\mathrm{LS}}\left(\Delta f_{\min}-\Delta f_{\mathrm{th}}\right)\right]\left(1+D\Delta f_{\min}\right)=0 \tag{29}$$

If the additional stage is shed, power balance when the residual frequency is reached is modeled as:

$$\left(1-P_{\mathrm{D\,max}}\right)-\left[1+K_{\mathrm{LS}}\left(\Delta f_{\min}-\Delta f_{\mathrm{th}}\right)+D\Delta f_{\mathrm{th}}\right]\left(1+D\Delta f_{\infty}\right)=0 \tag{30}$$

From (29), the following relationship can be found:

$$1+K_{\mathrm{LS}}\left(\Delta f_{\min}-\Delta f_{\mathrm{th}}\right)=\frac{1-P_{\mathrm{D\,max}}}{1+D\Delta f_{\min}} \tag{31}$$

Substitute (31) into (30), the minimum frequency is obtained as:

$$\Delta f_{\min} = \frac{\Delta f_{\infty}\left(1-P_{\mathrm{Dmax}}\right)+\Delta f_{\mathrm{th}}\left(1+D\Delta f_{\infty}\right)}{\left(1-P_{\mathrm{Dmax}}\right)-D\Delta f_{\mathrm{th}}\left(1+D\Delta f_{\infty}\right)} \tag{32}$$

Substitute (32) into (29), K_{LSmin} can be obtained with $\Delta f_{\infty}=\Delta f_{\mathrm{th}}$ as:

$$K_{\mathrm{LSmin}} = -\frac{P_{\mathrm{D\,max}}+D\Delta f_{\min}}{\left(\Delta f_{\min}-\Delta f_{\mathrm{th}}\right)\left(1+D\Delta f_{\min}\right)} \tag{33}$$

If P_{Dmax}=0.3, Δf_{th}=–0.01, and D=1, K_{LSmin} is 20.493 to make sure the system frequency can be successfully brought back to Δf_{th} and the maximum frequency deviation is –0.0238pu which is –1.190Hz for 50Hz systems or –1.428Hz for 60Hz systems.

Since system damping is changing with operating conditions, it is hard to track the precise value of D. The D used for tuning K_{LS} is usually chosen as typical value. It may be insufficient to tune K_{LS} as K_{LSmin} if uncertainties of operating conditions, voltage deviation and reduced boiler steam pressure are considered. A small positive gain α should be added to tune K_{LS} as follows to make the improved scheme adaptive to uncertainty:

$$K_{\mathrm{LS}} = \left(1+\alpha\right)K_{\mathrm{LSmin}} \tag{34}$$

α should be set according to the frequency dynamics. For different systems, α should be different and should be tuned to balance the frequency regulation performance and system economy. In this paper, α is set as 0.05 with several numerical simulations and is validated in section V. A greater α can be selected to increase K_{LS} if the frequency nadir is too low.

V. CASE STUDIES

The general performance of the proposed UFLS scheme is analyzed in section II and III with the simplified model. It is worthwhile to check the actual performance of the proposed scheme with detailed models. In this section, two systems are built with detailed models and tested with full time-domain simulation. One is 60Hz 39-bus New England model, and the other is 50Hz simplified Shandong Power Grid of China. System damping is modeled as load frequency dependency in the two systems. Therefore, K_{LS} is tuned as section IV.C.

A. Tests of New England model with steam turbines

In the New England model, the total load is 6150 MW and total generating capacity is 7300 MVA. All generators are modeled with 6-order GENROU generator model, IEEET1 exciter model, and IEEEG1 turbine-governor model[26]. Since load model is critical for power system dynamics[27], static IEELAL model with voltage and frequency dependency is used to model loads with typical parameters. The greatest power mismatch with N-2 contingency is 1830MW when tripping equivalent generators at bus 38 and 39. With system total load as base power, system D is 2.0, system R is 0.0421, and P_{Dmax} is 0.2975pu. Δf_{th} is set as –0.5Hz which is the activating frequency of the first stage of the stage-by-stage scheme. Thus, K_{LSmin} is calculated as 23.992 with (31). Final K_{LS} is tuned as 25.192 with α=0.05, i.e., shedding 41.987% load per Hz. The additional stage is set as P_{add}=–$D\Delta f_{\mathrm{th}}$=0.0167pu or 102.5MW. Time delay for the continuous part is t_{d}=0.2s, and time delay for the additional stage is t_{add}=10s. The traditional stage-by-stage UFLS scheme is listed in TABLE I [24] for comparison.

TABLE I. Stage-by-stage UFLS scheme of 39-bus New England model

Stage	1	2	3	4	5
Frequency/Hz	59.5	59.3	59.1	58.9	59.5
Time delay/s	0.3	0.3	0.3	0.3	10
Shedding percent	7%	7%	7%	7%	2.5%

COI frequency of tripping generator 38, 39, and tripping the two generators is shown in Fig. 12 with no spinning reserve. Loss of generation of the three events are: 830MW, 1000MW, and 1830MW. The same events with 10% spinning reserve are shown in Fig. 13. Nominal frequency and frequency threshold are shown in the two figures as dotted lines.

From Fig. 12 and 13, it can be found that both stage-by-stage and continuous scheme can bring system frequency back. However, in the zero spinning reserve scenario, system frequency will recover to greater than 60Hz for the event of tripping 830MW generation with the stage-by-stage scheme. Therefore, though the stage-by-stage scheme is well tuned, it still suffers from the over-shedding problem. The proposed continuous UFLS scheme, however, provides far better performance than the stage-by-stage scheme without any over-shedding problems.

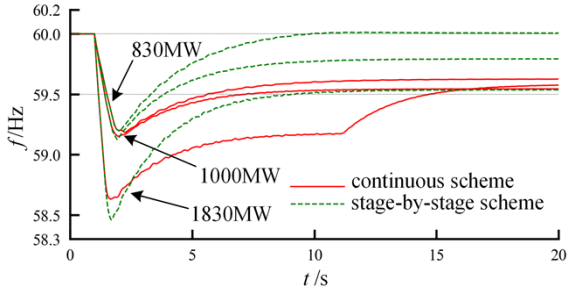

Fig. 12 Generator tripping events of New England model with no spinning reserve

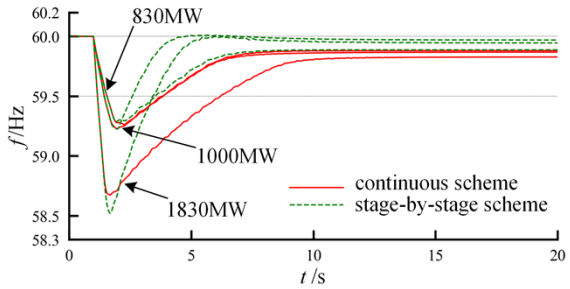

Fig. 13 Generator tripping events of New England model with 10% spinning reserve

Fig. 12 shows that the recovery speed of the frequency is relatively slow for the event of tripping 1830MW generation with the proposed scheme. A greater K_{LS} can be selected to avoid starting under-frequency protections of some power plants. Recovery speed can also be increased by adding other action logic to accelerate the operation of the additional stage according to the under-frequency protections of power plants.

To further check the voltage and angle stability, voltage and angle dynamics of the event of tripping generator 38 in Fig. 13 are illustrated in Fig. 14. It is shown that the voltage deviation is small and system is angular stable.

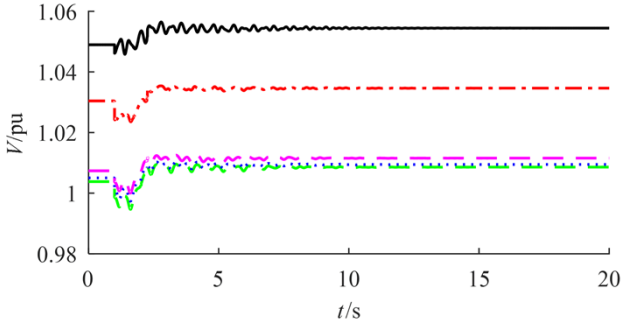

(a) Voltage dynamics

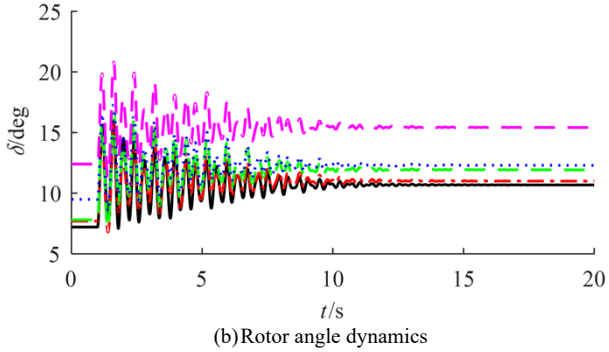

(b) Rotor angle dynamics

Fig. 14 Voltage and rotor angle dynamics of New England model with continuous scheme when generator 38 is tripped

The tuned continuous UFLS scheme is further implemented as three line-by-line schemes with 100, 50 and 20 low-voltage lines, i.e., each line uniformly carries 1%, 2%, and 5% of substation loads, respectively. The frequency response of the same events as Fig. 13 are illustrated in Fig. 15 to compare the line-by-line scheme with the continuous scheme. It can be found from Fig. 15 that though the line-by-line scheme is discrete, the three schemes implemented with precise load control can bring frequency back with similar performance as the continuous scheme.

To further check the adaptability of the continuous scheme, another continuous scheme is tuned as K_{LS}=28.790 with α=0.2, i.e., shedding 47.984% load per Hz. Results of the two schemes with K_{LS}=25.192 and K_{LS}=28.790 are shown in Fig. 16 with the same events as in Fig. 15. The scheme with K_{LS}=28.790 sheds loads slightly more than the scheme with K_{LS}=25.192 and reduce maximum frequency deviation by about 0.04Hz. The performance of the proposed continuous scheme is tolerant to change of α.

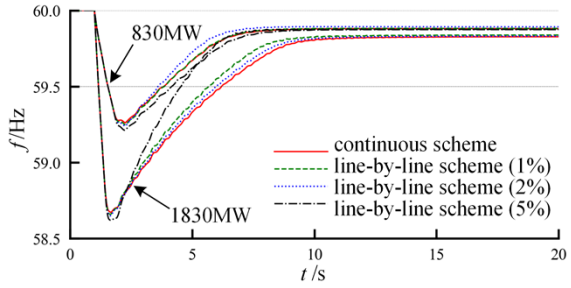

Fig. 15 Comparison of continuous and line-by-line schemes for generator tripping events of New England model with 10% spinning reserve

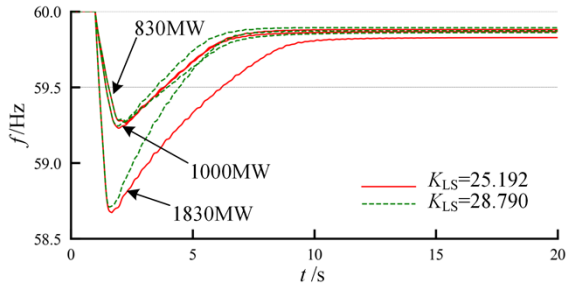

Fig. 16 Comparison of continuous schemes with different K_{LS} for generator tripping events of New England model with 10% spinning reserve

The proposed UFLS scheme is dependent on frequency dynamics which is affected by system inertia. To check the performance of the proposed scheme with different inertia, the New England model is tested with five cases, i.e., the base case, increasing H by 15% and 30%, and decreasing H by 15% and 30%, and results are shown in Fig. 17. It can be found that the proposed continuous UFLS scheme is adaptive to the change of system inertia.

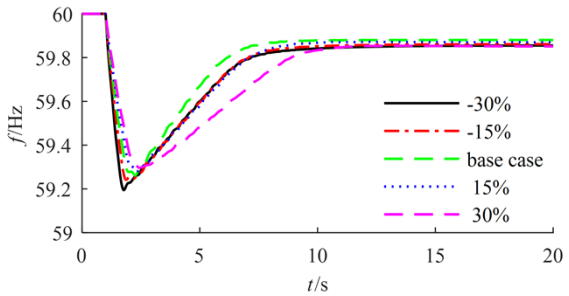

Fig. 17 Comparison of continuous schemes with different levels of system inertia with 10% spinning reserve

B. *Tests of Shandong Power Grid*

The simplified Shandong model consists of 118 buses with ten 1000kV buses and eighty-one 500kV buses, 24 generators, 31 transformers, 200 transmission lines, three high voltage direct current (HVDC) links, and 65 loads. The total load is 58.9GW. A ±660kV HVDC link is operated at 4GW and the other two ±800kV HVDC links are operated at 8GW each. Except for three generators modeled with classical GENCLS

model as sending units of the three HVDC links, other 21 generators are all modeled with GENROU generator model, SEXS exciter model, and TGOV turbine-governor model. All HVDC links are modeled with CDC4T model[26]. All loads are modeled with IEELAL model with voltage and frequency dependency. The traditional stage-by-stage scheme used in Shandong Power Grid is listed in TABLE II [25].

TABLE II. Stage-by-stage UFLS scheme of Shandong Power Grid

Stage	1	2	3	4	5	6	7	8
Frequency/Hz	49.25	49	48.75	48.5	48.25	48	47.75	49.25
Time delay/s	0.2	0.2	0.2	0.2	0.2	0.2	0.2	20
Shedding percent	4%	5%	6%	6%	6%	6%	6%	3%

The maximum power deficiency is 20GW or 33.97% when all HVDC links are blocked. The system damping is 2.0 based on system total load. With the proposed continuous UFLS scheme, K_{LSmin} is 14.130 when setting frequency threshold as 49.25Hz. With α=0.05, the K_{LS} is tuned as 14.837, i.e., shedding 29.674% load per Hz. The time delay of continuous load shedding part is 0.2. The additional stage is set to shed 3% of loads with a time delay of 10s.

When the system spinning reserve is 10% of total loads, the dynamic frequency is illustrated in Fig. 18 for events of blocking the ± 600kV HVDC link (4GW), one ± 800kV HVDC link (8GW), and all HVDC links (20GW). Fig. 18 verified that system frequency declination is arrested by both stage-by-stage and continuous UFLS schemes. In the stage-by-stage scheme, the frequency of 20GW event is reduced to 48.166Hz. The proposed continuous scheme, however, prevents system frequency from falling beyond 48.320Hz.

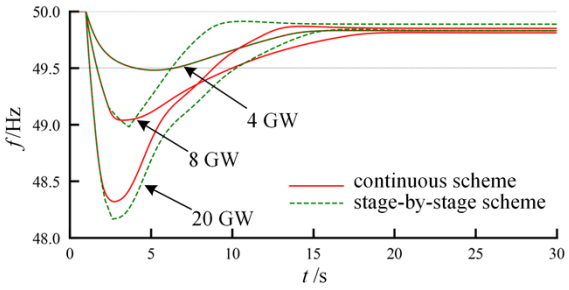

Fig. 18 Dynamic frequency of HVDC blocking events of Shandong Power Grid with 10% spinning reserve

Voltage and rotor angle dynamics when blocking all HVDC links of Fig. 18 is shown in Fig. 19. The system is stable with control of the continuous scheme.

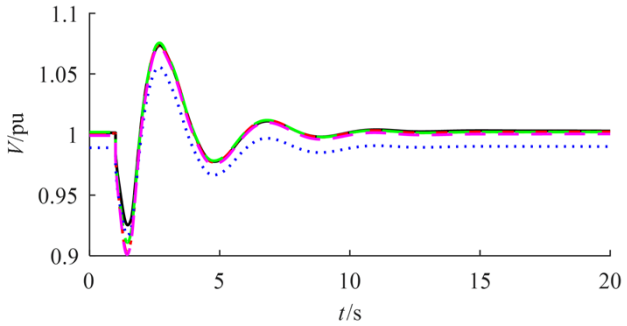

(a) Voltage dynamics

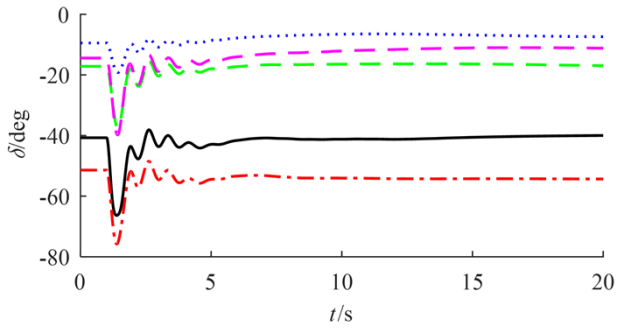

(b) Rotor angle dynamics

Fig. 19 Voltage and rotor angle dynamics of Shandong model with continuous scheme when all HVDC links are blocked

The line-by-line scheme is also checked with the same events as Fig. 18, and results are shown in Fig. 20. The three line-by-line schemes in Fig. 20 are valid to recover system frequency to the allowed range. Therefore, the line-by-line scheme is applicable in large-scale power systems.

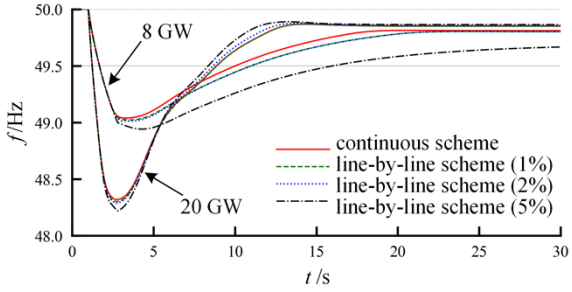

Fig. 20 Comparison of continuous and line-by-line schemes for HVDC blocking events of Shandong Power Grid with 10% spinning reserve

VI. DISCUSSIONS

In this paper, a continuous UFLS scheme is proposed to reinforce the performance of the response-driven emergency control. Besides the response-driven UFLS, event-driven emergency control is another important method to prevent severe frequency deviation, e.g., remedial action scheme (RAS) and system integrity protection scheme (SIPS). RAS and SIPS are set for specific contingencies and loads to shed are calculated according to the event signal to balance power deficiency. However, they can only deal with preset *N*-1 or *N*-2 contingencies. It is hard to set RAS and SIPS for other rare but severe *N*-*k* (*k*>2) contingencies due to the large amount of combination. For these contingencies, the response-driven UFLS can be started to prevent system collapse. Therefore, UFLS is backup of RAS and SIPS, and coordination between them need to be further studied in the future.

For the line-by-line scheme in the remote mode, additional communication channels are needed to transmit load information and tripping signal. The great investment and maintenance cost of communication infrastructures is the first obstacle for implementing the proposed UFLS scheme. To reduce the cost, communication channels can be shared with other applications. For example, the proposed UFLS scheme can use the same communication channels of RAS or SIPS to improve the utilization ratio of communication infrastructures.

For traditional stage-by-stage UFLS scheme, CBs on high-voltage lines are tripped when frequency drops beyond threshold. Important loads powered by the tripped lines will be

shed and the power supply reliability of distribution system operators (DSOs) is threatened. To improve the reliability of DSOs, the proposed UFLS scheme can be implemented to trip lines of lower-voltage level. Lines powering important loads can be labeled with high priority by DSOs and tripped as late as possible. It has potential to guarantee both frequency stability of transmission system operators (TSOs) and power supply reliability of DSOs. But the performance of the proposed scheme need to be further verified.

The theoretical performance of the proposed UFLS scheme is derived in section II based on the SFR model, in which only steam turbine is considered. However, there are other widely-used turbine governors, e.g., hydraulic, gas, combined-cycle wind, and etc. Dynamics of these turbine governors are different from that of steam turbine, and may affect the performance and tuning of the proposed UFLS scheme. Therefore, it is necessary to examine the adaptability of the propose UFLS scheme to the systems with other kinds of turbine governors in the future.

VII. Conclusions

UFLS is the key resort for preventing frequency collapse. With the development of new controllable devices and precise load control technique, power system frequency can be controlled in a smarter way than traditional stage-by-stage UFLS schemes. In this paper, a new continuous UFLS scheme is proposed to shed loads proportional frequency deviation. The proposed scheme is adaptive to power mismatch based on local measurement of frequency dynamics and is immune to the over-shedding problem. The improved continuous UFLS scheme incorporating frequency threshold and time delay is practical to implement and can be easily tuned with the proposed tuning method. The proposed UFLS scheme is adaptive to events and operating conditions. With precise load control, the continuous scheme can be implemented as the line-by-line scheme which can achieve similar performance as the continuous scheme.

References

[1] Y. Wen, C. Y. Chung and X. Ye, "Enhancing frequency stability of asynchronous grids interconnected with HVDC links," *IEEE Trans. on Power Systems*, vol. 33, no. 2, pp. 1800-1810, March 2018.

[2] P. Ferraro, E. Crisostomi, R. Shorten and et al., "Stochastic frequency control of grid-connected microgrids," *IEEE Trans. on Power Systems*, vol. 33, no. 5, pp. 5704-5713, Sept. 2018.

[3] Y. Liu, R. Fan and V. Terzija, "Power system restoration: a literature review from 2006 to 2016," *Journal of Modern Power System and Clean Energy*, vol.4, no.3, pp. 332-341, 2016

[4] N. Nguyen and J. Mitra, "An analysis of the effects and dependency of wind power penetration on system frequency regulation," *IEEE Trans. on Sustainable Energy*, vol. 7, no. 1, pp. 354-363, Jan. 2016.

[5] H. Golpîra, H. Seifi, A. R. Messina and et al., "Maximum penetration level of micro-grids in large-scale power systems: frequency stability viewpoint," *IEEE Trans. on Power Systems*, vol. 31, no. 6, pp. 5163-5171, Nov. 2016.

[6] B. Delfino, S. Massucco, A. Morini and et al., "Implementation and comparison of different under frequency load-shedding schemes," 2001 Power Engineering Society Summer Meeting, Vancouver, BC, Canada, 2001, pp. 307-312

[7] IEEE guide for the application of protective relays used for abnormal frequency load shedding and restoration," IEEE Std C37.117-2007, pp.1-55, 24 Aug. 2007

[8] X. Lin, H. Weng, Q. Zou and et al., "The frequency closed-loop control strategy of islanded power systems," *IEEE Trans. on Power Systems*, vol. 23, no. 2, pp. 796-803, May 2008.

[9] L. Sigrist, I. Egido, and L. Rouco. "A method for the design of UFLS schemes of small isolated power systems," *IEEE Trans. on Power Systems*, vol. 27, no. 2, pp. 951-958, 2012

[10] L. Zhang and J. Zhong, "UFLS design by using f and integrating df/dt," 2006 IEEE PES Power Systems Conference and Exposition, Atlanta, GA, 2006, pp. 1840-1844.

[11] T. Amraee, M. G. Darebaghi, A. Soroudi and et al., "Probabilistic under frequency load shedding considering RoCoF relays of distributed generators," *IEEE Trans. on Power Systems*, vol. 33, no. 4, pp. 3587-3598, July 2018.

[12] L. Sigrist, I. Egido and L. Rouco, "Performance analysis of UFLS schemes of small isolated power systems," *IEEE Trans. on Power Systems*, vol. 27, no. 3, pp. 1673-1680, Aug. 2012.

[13] V. V. Terzija, "Adaptive underfrequency load shedding based on the magnitude of the disturbance estimation," *IEEE Trans. on Power Systems*, vol. 21, no. 3, pp. 1260-1266, Aug. 2006.

[14] T. Shekari, F. Aminifar, and M. Sanaye-Pasand, "An analytical adaptive load shedding scheme against severe combinational disturbances," *IEEE Trans. on Power Systems*, vol. 31, no. 5, pp. 4135-4143, Sept. 2016.

[15] A. Ketabi and M. H. Fini, "An underfrequency load shedding scheme for hybrid and multiarea power systems," *IEEE Trans. on Smart Grid*, vol. 6, no. 1, pp. 82-91, Jan. 2015.

[16] L. Sigrist, I. Egido and L. Rouco, "Principles of a centralized UFLS scheme for small isolated power systems," *IEEE Trans. on Power Systems*, vol. 28, no. 2, pp. 1779-1786, May 2013.

[17] P. M. Anderson and M. Mirheydar, "An adaptive method for setting underfrequency load shedding relays," *IEEE Trans. on Power Systems*, vol. 7, no. 2, pp. 647-655, May 1992.

[18] P. M. Anderson and M. Mirheydar, "A low-order system frequency response model," *IEEE Trans. on Power Systems*, vol. 5, no. 3, pp. 720-729, Aug 1990.

[19] Y. Xie, H. Zhang, C. Li, et al. "Development approach of a programmable and open software package for power system frequency response calculation," *Protection and Control of Modern Power Systems*, vol.2, pp.189~198. 2017.

[20] M. A. Torres L., L. A. C. Lopes, L. A. Morán T. and et al., "Self-tuning virtual synchronous machine: a control strategy for energy storage systems to support dynamic frequency control," *IEEE Trans. on Energy Conversion*, vol. 29, no. 4, pp. 833-840, Dec. 2014.

[21] S. Acharya, M. S. E. Moursi and A. Al-Hinai, "Coordinated frequency control strategy for an islanded microgrid with demand side management capability," *IEEE Trans. on Energy Conversion*, vol. 33, no. 2, pp. 639-651, June 2018.

[22] W. Yin, Y. Yan, Q. Pan and et al., "Design of fast communication interface for precision load control system," *Automation of Electric Power Systems*, vol. 42, no. 10, pp. 143-149, 2018, in Chinese.

[23] H. Huang and F. Li, "Sensitivity analysis of load-damping characteristic in power system frequency regulation," *IEEE Trans. on Power Systems*, vol. 28, no. 2, pp. 1324-1335, May 2013.

[24] Northeast Power Coordinating Council, "NPCC regional reliability reference directory #12 under-frequency load shedding program requirements," https://www.npcc.org/Standards/Directories/Directory12%20Full%20Member%20clean%2020150330%20GJD.pdf, accessed on October 17, 2018.

[25] Y. Liu and C. Li, "Impact of large-scale wind penetration on transient frequency stability," 2012 IEEE Power and Energy Society General Meeting, San Diego, CA, 2012, pp. 1-5.

[26] Siemens, PSS/E model library V33.5, October 2013.

[27] V. Milanovic, J. Matevosyan, A. Gaikwad, et al. CIGRE WG C4.605: Modelling and aggregation of loads in flexible power networks. February 2014. https://e-cigre.org/publication/566-modelling-and-aggregation-of-loads-in-flexible-power-networks, accessed on April 10, 2019

Biography

Changgang Li (M'15) received the B.E. and Ph.D. degrees in Electrical Engineering from Shandong University, Jinan, China, in 2006 and 2012, respectively. He was a research scholar with the School of Electrical Engineering and Computer Science, the University of Tennessee, Knoxville, from 2012 to 2014. He is now an

Associate Research Fellow with the School of Electrical Engineering, Shandong University, China. His research interests are power system operation and control.

Yue Wu received the B.E. degree in Electrical Engineering from Zhengzhou University, Zhengzhou, China, in 2018. He is now a post-graduate student with Shandong University, China. His research interests are power system dynamic frequency control.

Yanli Sun received the B.E. and M.E. degree in Electrical Engineering from Shandong University, Jinan, China, in 2015 and 2018, respectively. She is now an engineer with State Grid Shandong Electric Power Corporation Weifang Power Supply Company, China. Her main research interests are power system analysis and control.

Hengxu Zhang (M'06) received the B.E. degree in Electrical Engineering from Shandong University of Technology, China, in 1998, and the M.S. and Ph.D. degrees in Electrical Engineering from Shandong University, China, in 2000 and 2003, respectively. He is now a Professor with the School of Electrical Engineering, Shandong University, China. His main research interests are power system security and stability assessment, power system monitoring, and numerical simulation.

Yutian Liu (SM'96) received the B.E. and M.S. degrees in electrical engineering from the Shandong University of Technology, Jinan, China, in 1984 and 1990, respectively, and the Ph.D. degree in electrical engineering from Xi'an Jiaotong University, Xi'an, China, in 1994. He is currently a Chair Professor at the School of Electrical Engineering, Shandong University, Jinan. His research interests include power system analysis and control, renewable energy integration, and artificial intelligence application to power system

Yilu Liu (S'88–M'89–SM'99–F'04) received her M.S. and Ph.D. degrees from the Ohio State University, Columbus, in 1986 and 1989. She received the B.S. degree from Xian Jiaotong University, China. Dr. Liu is currently the Governor's Chair at the University of Tennessee, Knoxville and Oak Ridge National Laboratory (ORNL). Dr. Liu is elected as the member of National Academy of Engineering in 2016. She is also the Deputy Director of the DOE/NSF cofunded engineering research center CURENT. Prior to joining UTK/ORNL, she was a Professor at Virginia Tech. She led the effort to create the North American power grid frequency monitoring network (FNET) at Virginia Tech, which is now operated at UTK and ORNL as GridEye. Her current research interests include power system wide-area monitoring and control, large interconnection-level dynamic simulations, electromagnetic transient analysis, and power transformer modeling and diagnosis.

Vladimir Terzija (M'95-SM'00-F'16) is the EPSRC Chair Professor in Power System Engineering in the School of Electrical and Electronic Engineering, the University of Manchester, U.K., where he has been since 2006. From 1997 to 1999, he was an Assistant Professor at the University of Belgrade, Serbia. From 2000 to 2006, he was with ABB AG, Germany, working as an expert for switchgear and distribution automation. His main research interests are Smart Grid, application of intelligent methods to power system monitoring, control, and protection, switchgear and fast transient processes, as well as DSP applications in power systems.